WEDNESDAY SLIDE CONFERENCE 2022-2023

Conference #3   **31 August 2022**

CASE I:

Signalment:
2-year-old, male, C57/BL6 CuZnSOD wild type (*Mus musculus*)

History:
This mouse recently arrived at the facility and was housed in quarantine. Two days after arrival the mouse presented clinically with abdominal distension. On physical examination, a large abdominal mass was palpated, and humane euthanasia was elected.

Gross Pathology:
The mouse was in fair body condition (BCS 2.5/5). The lungs were mottled with patchy pale yellow to pink foci. Within the abdomen, there were three encapsulated masses associated with the mesentery that ranged in size from 0.5-2cm in diameter (gross photo, black asterisks). On cut section, the masses were abscessed. The liver and the spleen were diffusely enlarged.

Laboratory Results:
No laboratory findings reported.

Microscopic Description:
Throughout all lung lobes there are multifocal to coalescing inflammatory infiltrates filling alveolar spaces. Inflammatory infiltrates are primarily composed of large plump macrophages and multinucleated giant cells admixed with eosinophils and fewer lymphocytes, plasma cells, and neutrophils. Macrophages and multinucleated giant cells contain abundant intracytoplasmic brightly eosinophilic partially refractile acicular to rectangular crystals admixed with homogenous eosinophilic hyalinized material. Crystals and hyaline are also present within in the extracellular space. There are perivascular and peribronchiolar lymphoplasmacytic cuffs.

In the section of liver, there is marked proliferation of myeloid precursors primarily surrounding portal regions. Myeloid precursors
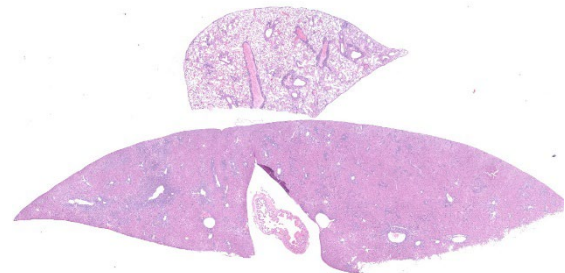
Figure 1-1. Lung, liver, mouse. A section of lung and liver are submitted for examination. At subgross magnification, there is diffuse expansion of peribronchiolar and perivascular areas by a cellular infiltrate and a focally extensive area of subpleural inflammation; the liver demonstrates expansion of portal areas and focally extensive thickening of the gallbladder mucosa. (HE, 7X)
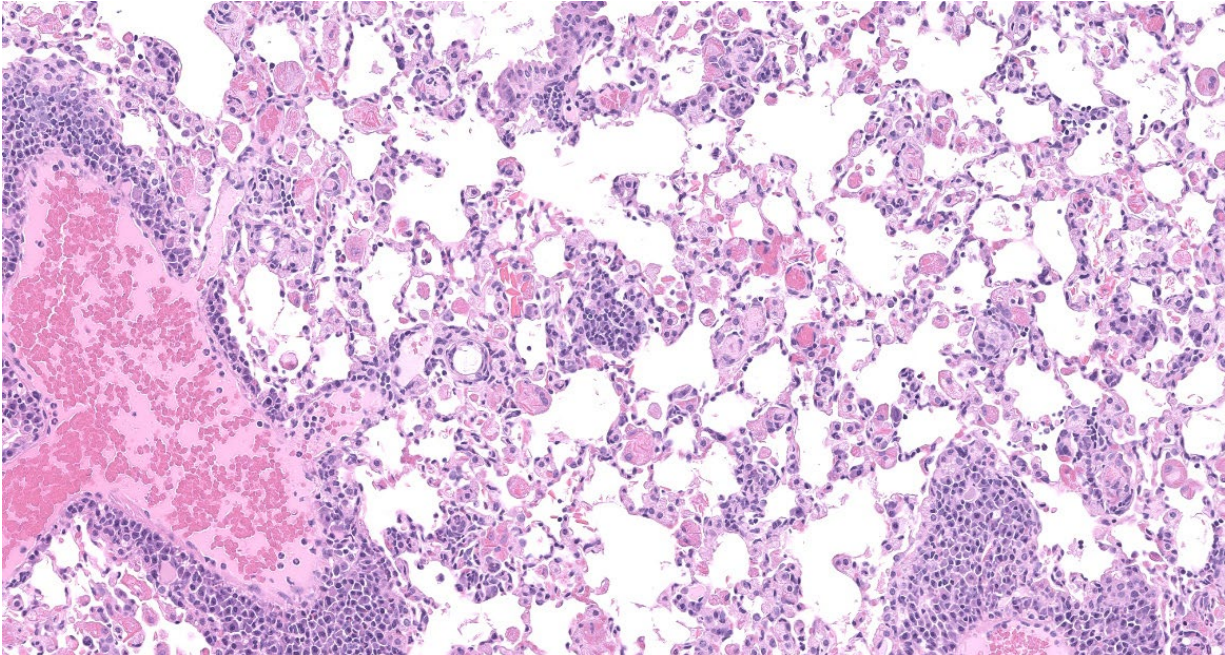
Figure 1-2. Lung, mouse. Alveolar lumina contain scattered aggregates of swollen eosinophilic macrophages and occasional large extracellular eosinophilic crystals; there are numerous plasma cells and fewer lymphocytes and macrophages in perivascular areas. (HE, 181X)

infiltrate into the parenchyma and bridge adjacent portal tracts. Hepatic cords are attenuated. The biliary and gall bladder epithelium are expanded by intracytoplasmic eosinophilic hyalinized material. There are acicular and rectangular crystals within the gall bladder.

Contributor's Morphologic Diagnoses:
Lung: Eosinophilic and granulomatous pneumonia, chronic, severe, with eosinophilic crystals.
Liver and spleen: Myeloid hyperplasia, marked, diffuse.
Bile ducts/gall bladder: Epithelial hyalinosis, marked, multifocal.

Contributor's Comment:
Eosinophilic crystalline pneumonia (ECP), also known as acidophilic macrophage pneumonia, is a common age-related background lesion in C57/BL6 and 129/Sv mice and in many of their knockout and transgenic derivatives.[5,7,9] This lesion can be exacerbated during concurrent pulmonary disease, and has been reported in association with systemic infectious, neoplastic, hypersensitivity, and lymphoproliferative disorders.[5] Eosinophilic crystals are derived from macrophages and are primarily composed of iron, alpha-1 antitrypsin, immunoglobulin, and granulocyte breakdown products.[2,6] In addition to accumulation within macrophages and the lung, this protein can also accumulate within epithelial cells of the pancreas, stomach, liver and gallbladder, and the olfactory epithelium.[2,4] Of note, in addition to ECP and epithelial hyalinosis, this mouse also had multiple abdominal abscesses and myeloid hyperplasia in the spleen, kidney, and liver. Thus, it was determined that the severe ECP in this case was likely due to age and exacerbated by chronic systemic inflammation.

Contributing Institution:
In Vivo Animal Core, University of Michigan, Unit for Laboratory Animal Medicine
https://animalcare.umich.edu/business-services/vivo-animal-core
ulam-ivac@umich.edu
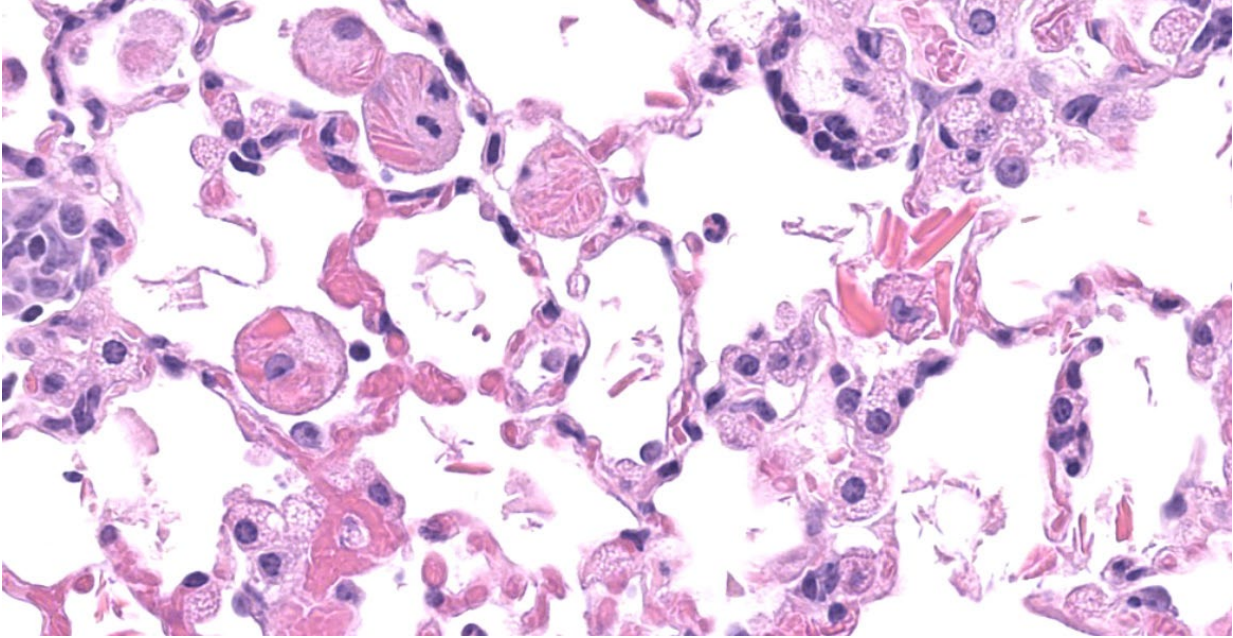
Figure 1-3. Lung, mouse. Macrophages contain large oblong to needle-shaped eosinophilic crystals within their cytoplasm; similar crystals are also freely present in the alveolar lumina. (HE, 715X)

JPC Diagnoses:

1. Lung: Alveolitis, granulomatous, diffuse, moderate, with intrahistiocytic and extracellular eosinophilic crystals and perivascular plasmacytosis.
2. Liver, gallbladder: Biliary epithelial hyalinosis and extracellular crystals, diffuse, severe.
3. Liver: Extramedullary hematopoiesis, diffuse, severe.

JPC Comment:

As the contributor mentions, eosinophilic crystalline pneumonia occurs regularly in aged B6 mice and has a more rapid onset in the moth-eaten phenotype of B6 mice.[2] Moth-eaten strains have a deficiency of Shp1, a protein tyrosine phosphatase involved in the immune signaling pathways of multiple hematopoietic cell types, due to a spontaneous mutation of Ptpn6.[1] In the lung, Shp1 deficiency is associated with the rapid accumulation of eosinophilic crystals within pulmonary macrophages, while in the skin, Shp1 deficiency results in neutrophilic inflammation and dendritic-cell driven autoimmunity

producing chronic dermatitis and alopecia, the basis of the "moth-eaten" designation.[1,10] Other strains which are predisposed to hyalinosis include female CYP1A2-null mice and female 129S4/SvJae mice, with one study documenting hyalinosis of the glandular stomach in over 95% and 45% of these strains, respectively.[10] These mice had grossly visible plaque-like lesions in the cardia; histologically, there was disorganization, hyperplasia, and hyalinization of gastric epithelial cells and abundant extracellular eosinophilic crystals.[10]

Grossly, ECP causes firm pale tan lesions in the lung which fail to collapse.[8] Affected
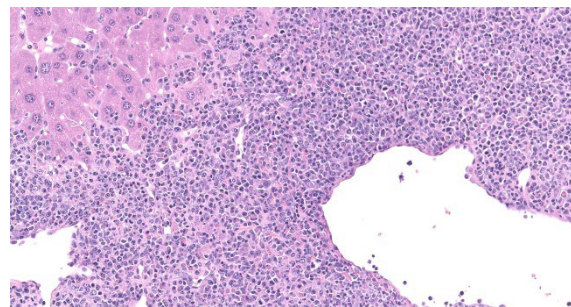
Figure 1-4. Liver, mouse. There is marked extramedullary hematopoiesis within perivascular areas on the liver. (HE, 247X)
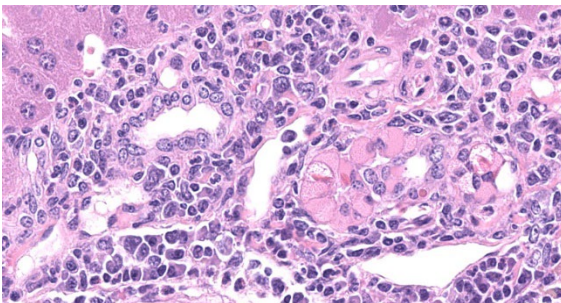
3

gallbladders may have mural thickening and opacification with bile duct fibrosis.[10]

In addition to the components listed by the contributor, eosinophilic crystals contain Ym1 (eosinophilic chemotactic factor) and Ym2, two closely related chitinases with different patterns of distribution throughout the body.[2,10] Pulmonary lesions primarily contain Ym1, and other organ systems contain a mixture of both Ym1 and Ym2.[2]
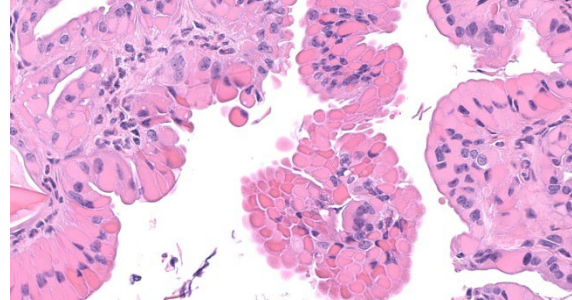
Differential diagnoses for ECP include pulmonary histiocytosis, which typically occurs in the subpleural regions, or alveolar lipoproteinosis, may contain granular eosinophilic material (surfactant) and scattered macrophages.[2] Hemorrhage can lead to extracellular hemoglobin crystal formation.[2,3] Eosinophilic crystals have also been seen in particulate inhalation studies, *Cryptococcus neoformans* infections in mice, and some dietary toxicity and drug studies in rats.[3]

References:
1. Abram CL, Roberge GL, Pao LI, Neel BG, Lowell CA. Distinct roles for neutrophils and dendritic cells in inflammation and autoimmunity in motheaten mice. *Immunity*. 2013;38: 489-501.
2. Barthold SW, Griffey SM, Percy DH. Pathology of Laboratory Rodents and Rabbits. 4th ed. Ames, IO: Wiley Blackwell; 2016: 3,94-95,100.

Figure 1-6. Gallbladder, mouse. Gallbladder epithelium is segmentally expanded by epithelium with pink to bright red cytoplasmic granules. (HE, 520X)

3. Cesta MF, Dixon D, Herbert RA, Staska LM. Lung – Crystals. US Department of Health and Human Services National Toxicology Program Nonneoplastic Lesion Atlas. Accessed 11 August 2022. https://ntp.niehs.nih.gov/nnl/respiratory/lung/crystal/index.htm
4. Giannetti N, Moyse E, Ducray A, et al. Accumulation of Ym1/2 protein in the mouse olfactory epithelium during regeneration and aging. *Neuroscience*. 2004;123: 907-917.
5. Hoenerhoff MJ, Starost MF, Ward JM. Eosinophilic crystalline pneumonia as a major cause of death in 129S4/SvJae mice. *Vet Pathol*. 2006;43(5).
6. Klug JJ, Snyder JM. Eosinophilic crystalline pneumonia, an age-related lesion in mice. *Aging Pathobiol Ther*. 2020;2: 232-233.
7. Murray AB, Luz A. Acidophilic Macrophage Pneumonia in Laboratory Mice. *Vet Pathol*. 1990;27(4).
8. Pettan-Brewer C, Treuting PM. Practical pathology of aging mice. *Pathobiol Aging Age Relat Dis*. 2011;1.
9. Radaelli E, Castiglioni V, Recordati C, et al. The Pathology of Aging 129S6/SvEv-Tac Mice. *Vet Pathol*. 2016;53(2): 477-492.
10. Ward JM, Yoon M, Anver MA, et al. Hyalinosis and Ym1/Ym2 Gene Expression in the Stomach and Respiratory Tract of 129S4/SvJae and Wild-Type and

Figure 1-5. Liver, mouse. Multifocally, biliary epithelium in portal areas is markedly swollen with eosinophilic cytoplasmic granules. (HE, 720X)

CYP1A2-Null B6,129 Mice. *Am J Pathol.* 2001; 158(1):323-332.

11. Zhao T, Su Z, Li Y, Zhang X, You Q. Chitinase-3 like-protein-1 function and its role in diseases. *Signal Transduct Target Ther.* 2020;5: 201.

CASE II:

Signalment:
18-month-old male, *Apoe^tm1Unc* KO on C57BL/6 background (*Mus musculus*)

History:
This mouse was part of an atherosclerosis study and was transitioned to a Western high fat diet at 3-months of age. At 15-months, the mouse became pruritic and developed ulcerative dermatitis that wax and waned despite treatment. Humane euthanasia was elected at 18-months.

Gross Pathology:
The mouse was overly conditioned with a body condition score of 5/5. On external examination, there were deep skin erosions and ulcers on the right flank and left right forelimb that ranged in size from 1-4mm in diameter. The liver was diffusely enlarged and friable. The submandibular and renal lymph nodes were enlarged. The remainder of the postmortem examination was within normal limits.

Laboratory Results:

Figure 2-1. Heart and pinna, mouse. At subgross magnification, the pinna wall is markedly expanded and normal architecture is lost. (HE, 7X)
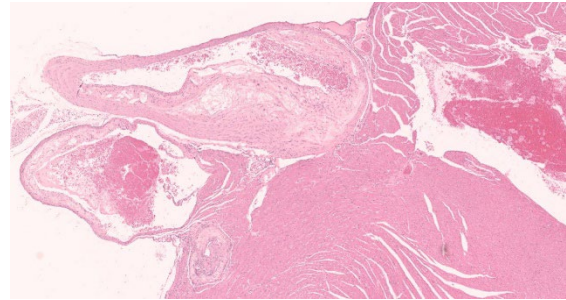
Figure 2-2. Heart base, mouse. The walls of the aorta, pulmonary artery and a subjacent coronary artery are segmentally to circumferentially expanded by lipid, forming clear clefts within the tunica intima and media. The lumen of the coronary artery is recanalized. (HE, 35X)

No laboratory findings reported.

Microscopic Description:
The aorta and pulmonary artery are segmentally narrowed due to luminal expansion by atherosclerotic subintimal plaques. Subintimal plaques occasionally extend into the tunica media and are composed of diffuse aggregates of acicular cholesterol cleft, plump foamy macrophages, multinucleated giant cells, and lymphocytes. There are rare foci of dystrophic mineralization and fibrosis.

In multiple sections of skin, the epidermis is necrotic and ulcerated and the dermis is expanded by granulation tissue which supports abundant acicular cholesterol clefts, plump foamy macrophages, multinucleated giant cells, and fewer lymphocytes and plasma cells. Inflammation and cholesterol deposits extend from the superficial dermis into the deep muscular layers and subcutis. Inflammation occasionally encompasses nerve bundles and skeletal muscle myofibers are atrophied. Adjacent to the ulcers the epidermis is acanthotic and there are superficial serocellular crusts.

Contributor's Morphologic Diagnoses:
Heart (pulmonary artery, aorta, and vessels): Atherosclerosis, segmental, moderate.
Skin: Ulcerative dermatitis with dermal xanthomatosis, chronic, multifocal, severe.
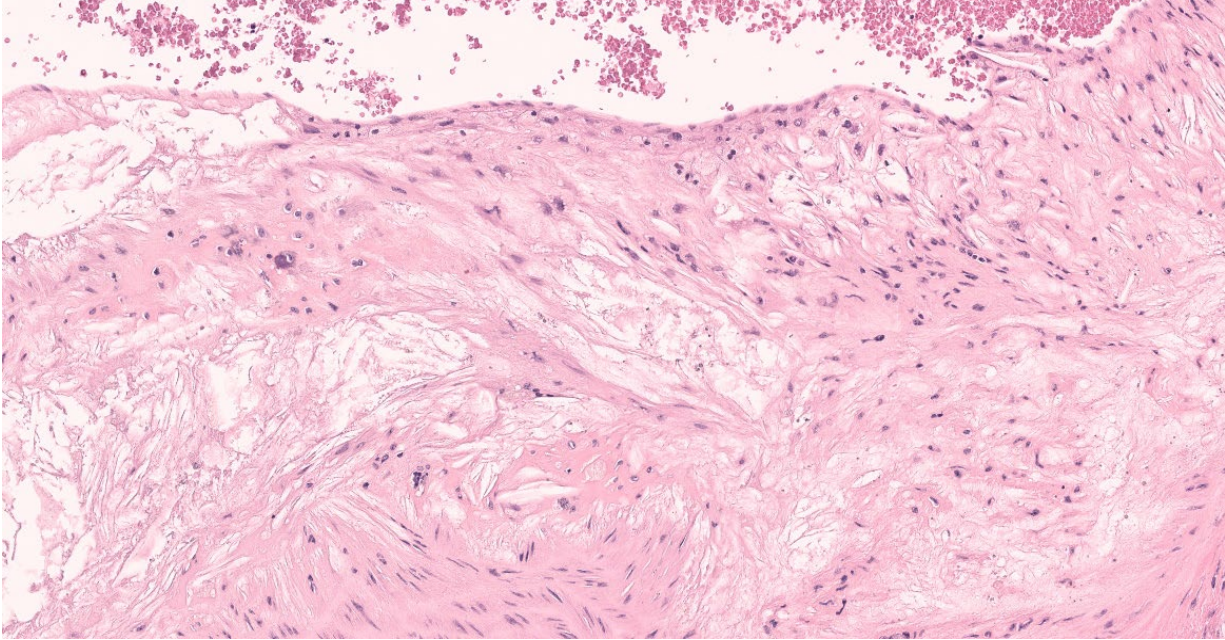
Figure 2-3. Aorta, mouse. There is marked disorganization of the aortic tunica intima and media. The wall is expanded by clefts of lipid and there is loss of the tunica intima, marked smooth muscle disarray, and fibrosis. (HE, 163X)

Contributor's Comment:

Apolipoprotein E deficient (ApoE^{-/-}) mice are useful for the study of mechanisms underlying cardiovascular disease and atherosclerosis, fat metabolism, and neurodegenerative diseases.[3,8,16] ApoE is a structural component of lipoproteins that regulates lipid homeostasis and facilitates lipid transport. It functions as a ligand in the transport of many lipid products, such as cholesterol and fat-soluble vitamins, between cells and tissue.

Hypercholesterolemia is the primary clinical pathology finding characteristic of ApoE^{-/-} mice.[20] Subsequently, atherosclerosis and multicentric xanthomas (lipid mass-like accumulations) are well-recognized phenotypes of this model. Indeed, ApoE^{-/-} mice can develop pre-atherosclerotic lesions, such as subintimal fatty streaks, in the proximal aorta as early as 3-months of age.[16] Of interest to the current case, chronic hypercholesterolemia can alter epidermal lipid composition which may impair innate immune defense barriers of the skin which is associated with foam cell deposition in the dermis in both humans and in mice.[1,9] Further, ApoE^{-/-} mice fed a hypercholesterolemic diet exhibited xanthomatosis in many organs with a predilection for the subcutaneous and peritendinous tissues, similar to the skin lesions presented in this case. However, the ulcerative epidermal component in this mouse is somewhat unique.[18] Given the C57/BL6 background idiopathic ulcerative dermatitis (UD), a commonly reported entity associated with pruritis in aging C57/BL6 mice, was considered as a top differential clinically. Indeed, wild type C57/BL6 mice fed a high-fat diet had worsened UD lesions compared to mice on standard rodent chow.[5] In this case, it is suspected the implementation of a high fat diet exacerbated the lipogranulomatous dermal lesion and the presence of inflammation around nerve bundles may have contributed to the pruritis and subsequent ulcerative dermatitis noted clinically; however, initial UD may have also played a primary role. In conclusion, the clinical and histopathologic features of both ulcerative dermatitis and dermal xanthomatosis were considered in this case. The underlying etiologies of the skin lesion
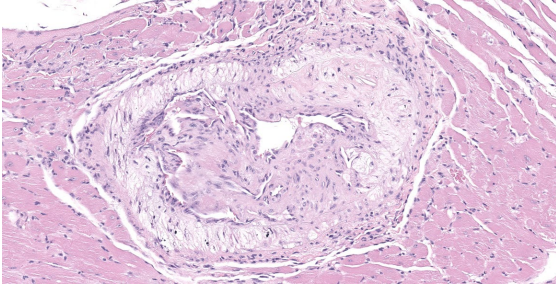
Figure 2-4. Coronary artery, mouse. Similar changes are present in the wall of the coronary artery. Smooth muscle cells also contain cytoplasmic lipid. There is re-canalization of the lumen with marked fibrosis of the tunica intima. (HE, 226X)

are thought to be driven by the genotype and further potentiated by both the high fat diet and UD.

Contributing Institution:
In Vivo Animal Core, University of Michigan, Unit for Laboratory Animal Medicine
https://animalcare.umich.edu/business-services/vivo-animal-core
ulam-ivac@umich.edu

JPC Diagnoses:
1. Heart, arteries: Atherosclerosis, multifocal, marked.
2. Heart, left ventricle: Fibrosis, subendocardial, multifocal, mild to moderate, with cardiomyocyte degeneration and loss.
3. Ear pinna: Dermatitis, xanthogranulomatous, diffuse, marked with multifocal epidermal ulceration.

JPC Comment:
The term xanthoma is derived from *xanthos*, the Greek word for yellow.[19] Xanthomas have been reported in numerous veterinary species and are relatively common in birds, less common in cats, and rare in dogs, horses, amphibians, and reptiles.[13,14,15,17,19] Of the avian species, older psittacines are the most commonly affected, and lesions may occur in the skin of the abdomen, wings, and eyelids, with rare involvement of internal organs such as the bone marrow, liver, and ventricu-

lus.[15,17] In birds, dermal xanthomas are variably inflamed, often pruritic nodular masses that lead to self-mutilation. Chronic irritation, trauma, and high fat/high cholesterol diets are associated with xanthoma development in birds. In mammals, xanthomas may also be caused by high lipid diets, defective lipid metabolism, or underlying endocrine dysfunction (such as diabetes mellitus, hypothyroidism, hypoadrenocorticism, and pituitary pars intermedia dysfunction in horses).[19] In dogs, a rare but striking form of xanthoma can occur in the eye secondary to the previously listed causes or lens-induced uveitis; grossly, affected eyes may be filled with yellow-tan material.[7]

Xanthomas in the central nervous system can lead to neurologic signs secondary to compression of adjacent parenchyma. In dogs, xanthogranulomas have rarely been reported in the sellar region. One recent report described xanthogranuloma intimately associated with a functional pituitary adenoma in a dog with hyperadrenocorticism and hypoparathyroidism; while the clinical signs in this case were attributed to the functional pituitary adenoma, another report described neurologic changes including aggression, seizures, and proprioceptive deficits due to compression by a xanthogranuloma in the pituitary region of a poodle with hyperadrenocorticism and hypothyroidism.[2] A similar lesion, termed cholesteatoma, occurs in the choroid plexus of older horses secondary to recurrent mild hemorrhage.[11] Large cholesteatomas obstruct the flow of cerebrospinal fluid causing secondary hydrocephalus.[11]

Buildup of lipid, lipid-laden macrophages, and cholesterol crystals in the tunica intima of large arteries, as demonstrated in this case, is termed atherosclerosis. Atherosclerosis is one of the most important diseases of humans

and is a leading cause of mortality due to resulting myocardial infarction, cerebral infarction, aneurysm, and peripheral vascular disease. The complex pathogenesis involves a combination of hypercholesterolemia, endothelial dysfunction, and chronic inflammation.[12] Intimal plaques occur in areas of turbulent blood flow and endothelial dysfunction and are initially composed of lipid-laden smooth muscle cells and macrophages. Extracellular oxidized LDL (generated by reactive oxygen species from previously activated macrophages) and phagocytosed cholesterol and fatty acids stimulate inflammasome formation, IL-1 production, and further activation of macrophages and T cells, perpetuating the inflammation. Cytokines and growth factors stimulate smooth muscle proliferation and collagen production, expanding the intimal plaque and creating a fibrous cap on the luminal surface. The plaque contains a core of lipid, lipid-laden cells, and possibly mineral, and if the fibrous cap is unstable and ruptures, this material is released into the vessel, causing thrombosis with vessel occlusion or embolization. Alternatively, outward pressure of the growing plaque can weaken the tunica media, resulting in aneurysm. Chronic atherosclerosis can also lead to gradual stenosis in smaller arteries, such as the coronary arteries, eventually resulting in tissue ischemia.

Clinical atherosclerosis in veterinary species is exceedingly rare, which creates a challenge when searching for animal models in this important human disease. Chickens, parrots, rabbits, pigs, and primates are susceptible to atherosclerosis, and while cats are generally considered atheroresistant, a recent report described clinical atherosclerosis in two related Korat breed cats with progressive cardiovascular failure.[6] The histologic lesions were nearly identical to those seen in humans, and both had chronic myocarditis and fibrosis likely secondary to coronary artery stenosis and myocardial ischemia. In experimental models, pigs, rabbits, non-human primates, and mice are currently used, with the mouse being the most popular model in part due to its relative low cost and ease of genetic manipulation.[4] ApoE or LDL deficient mouse models have provided tremendous insight
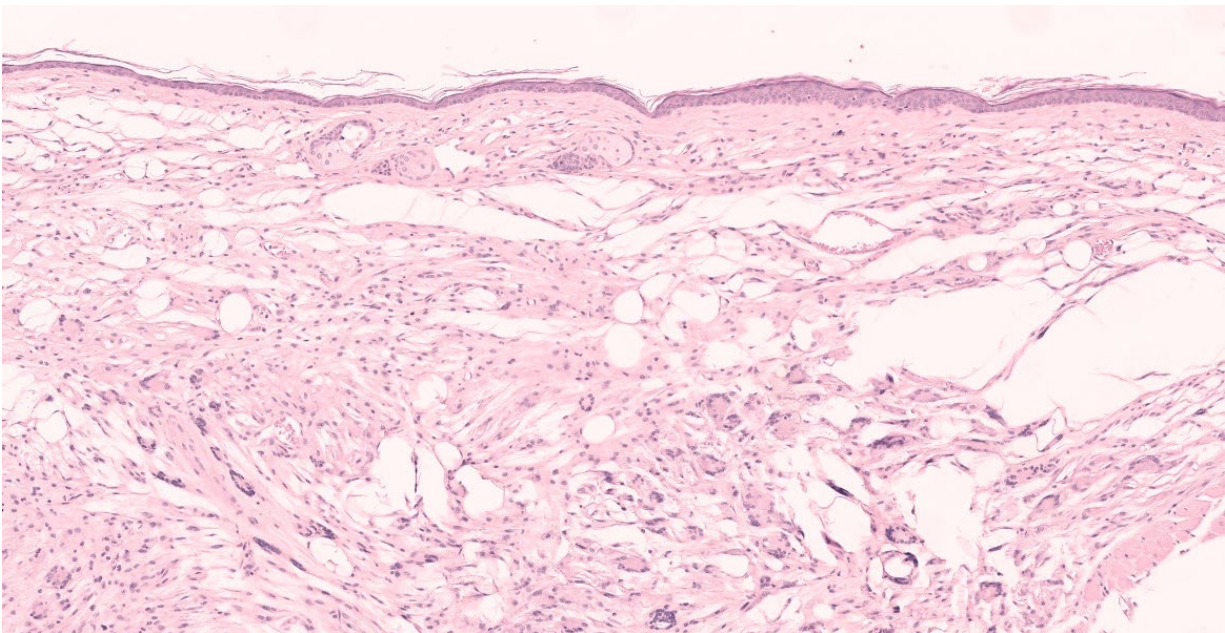
Figure 2-5. Pinna, mouse. The dermis is markedly expanded by acicular lipid either free in the tissue or surrounded by multi-nucleated giant cell macrophages. (HE, 98X)

into atherogenesis, but even they do not perfectly recapitulate the human disease, as they lack coronary stenosis and plaque instability.[4]

References:

1. Bedja D, Yan W, Lad V, et al. Inhibition of glycosphingolipid synthesis reverses skin inflammation and hair loss in ApoE−/− mice fed western diet. *Sci Rep.* 2018;8(1).

2. Fernandez-Gallego A, Del-Pozo J, Boag A, Maxwell S, Perez-Acino J. Xanthogranulomatous Pituitary Adenoma in a Dog with Typical Hyperadrenocorticism. *J Comp Pathol.* 2020;180**:** 115-121.

3. Gao J, Katagiri H, Ishigaki Y, et al. Involvement of apolipoprotein E in excess fat accumulation and insulin resistance. *Diabetes.* 2007;56(1).

4. Getz GS, Reardon CA. Animal models of atherosclerosis. *Arterioscler Thromb Vasc Biol.* 2012;32**:** 1104-1115.

5. Hampton AL, Aslam MN, Naik MK, et al. Ulcerative dermatitis in C57BL/6NCrl mice on a low-fat or high-fat diet with or without a mineralized red-algae supplement. *J Am Assoc Lab Anim Sci.* 2015;54(5).

6. Karkamo V, Airas N, Linden J, et al. Severe Spontaneous Atherosclerosis in Two Korat Breed Cats is Comparable to Human Atherosclerosis. *J Comp Pathol.* 2021;188**:** 52-61.

7. Labelle P. The Eye. In: Zachary JF, ed. *Pathologic Basis of Veterinary Disease.* 7th ed. St. Louis, MO: Elsevier, Inc; 2021: 1429.

8. Lewandowski CT, Maldonado Weng J, LaDu MJ. Alzheimer's disease pathology in APOE transgenic mouse models: The Who, What, When, Where, Why, and How. Neurobiol Dis. 2020;139. doi:10.1016/j.nbd.2020.104811

9. Martins Cardoso R, Creemers E, Absalah S, et al. Hypercholesterolemia in young adult APOE −/− mice alters epidermal lipid composition and impairs barrier function. Biochim Biophys Acta - Mol Cell Biol Lipids. 2019;1864(7).

10. Mitchell RN, Halushka MK. Blood Vessels. In: Kumar V, Abbas AK, Aster JC, eds. *Robins & Cotran Pathologic Basis of Disease.* 10th ed. Philadelphia, PA: Elsevier, Inc; 2021: 493-504.

11. Miller AD, Porter BF. Nervous System. In: Zachary JF, ed. *Pathologic Basis of Veterinary Disease.* 7th ed. St. Louis, MO: Elsevier, Inc; 2021: 966.

12. Oakes SA. Cell Injury, Cell Death, and Adaptations. In: Kumar V, Abbas AK, Aster JC, eds. *Robins & Cotran Pathologic Basis of Disease.* 10th ed. Philadelphia, PA: Elsevier, Inc; 2021: 62-63.

13. Origgi FC. Lacertilia. In: Terio KA, McAloose D, St. Leger J, edgs. *Pathology of Wildlife and Zoo Animals.* Cambridge, MA: Elsevier, Inc: 2018: 879.

14. Pessier AP. Amphibia. In: Terio KA, McAloose D, St. Leger J, edgs. *Pathology of Wildlife and Zoo Animals.* Cambridge, MA: Elsevier, Inc: 2018: 927.

15. Reavill DR, Dorrestein G. Psittacines, Coliiformes, Musophagiformes, Cuculiformes. In: Terio KA, McAloose D, St. Leger J, edgs. *Pathology of Wildlife and Zoo Animals.* Cambridge, MA: Elsevier, Inc: 2018: 782.

16. Reddick RL, Zhang SH, Maeda N. Atherosclerosis in mice lacking Apo E - Evaluation of lesional development and progression. *Arterioscler Thromb Vasc Biol.* 1994;14(1).

17. Schmidt RE, Reavill DR, Phalen DN. *Pathology of Pet and Aviary Birds.* 2nd ed. Ames, IO: John Wiley & Sons, Inc; 2015. 73, 116, 194, 260, 264.

18. van Ree JH, Gijbels MJJ, van den Broek WJAA, Hofker MH, Havekes LM. Atypical xanthomatosis in apolipoprotein E-

deficient mice after cholesterol feeding. Atherosclerosis. 1995;112(2).

19. Welle MM, Linder KE. The Integument. In: Zachary JF, ed. *Pathologic Basis of Veterinary Disease*. 7th ed. St. Louis, MO: Elsevier, Inc; 2021: 1190, 1219.

20. Zhang SH, Reddick RL, Piedrahita JA, Maeda N. Spontaneous hypercholesterolemia and arterial lesions in mice lacking apolipoprotein E. *Science* (80-). 1992;258(5081).

CASE III:

Signalment:
2 year old, female intact, Domestic Shorthair cat (*Felis catus*)

History:
This cat presented to the primary veterinarian following acute decline at home over the previous 24 hours, characterized by acute inappetence, lethargy, labored breathing, an enlarged left submandibular lymph node, abnormal urination and defecation, and hiding behavior. The cat had been acting normally prior to the decline and no vomiting, diarrhea, coughing or sneezing were noted. The cat was indoor only and had been previously vaccinated but was not up to date. It was living with three more cats, none of whom displayed abnormal clinical signs. On physical examination, the cat was lethargic, bradycardic (130 beats/min), and tachypneic (90

Figure 3-1. Multiple sections of lung are submitted for examination, with up to 100% effacement of pulmonary architecture by a dense cellular infiltrate. (HE, 7X)

breaths/min) with an audible wheeze and increased abdominal effort. The left submandibular lymph node was markedly enlarged to approximately 2 cm in diameter, while the remaining peripheral lymph nodes palpated normal. The cat was afebrile and had no obvious oral lesions.

A complete blood count (CBC) and blood smear revealed a marked leukopenia, driven by marked neutropenia and lymphopenia. FeLV and FIV testing was negative. Thoracic radiographs revealed multiple nodular soft tissue opacities throughout the lung fields, ranging in size from 0.2 cm to greater than 1.0 cm. Advanced pulmonary metastatic disease was suspected, with bacterial or fungal granuloma considered less likely.
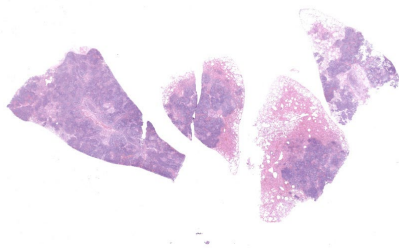
The cat was euthanized due to the need for aggressive intervention and a guarded prognosis.

Gross Pathology:
Affecting approximately 60-70% of the total surface area of the lungs were numerous, occasionally coalescing, well demarcated, raised, slightly firm, irregularly circular, beige to dark brown masses surrounded by a thin beige rim. The masses ranged from 0.4 cm to 1.9 cm in diameter, extended deep into the lung parenchyma, and had a bulging, granular appearance on cut surface. Overall, the lungs were mottled red to dark red, wet, heavy, and oozed a small to moderate amount of red, clear, watery fluid and a small amount of pink-tinged froth on cut section. There were multiple, friable, weak adhesions between the lung lobes and the adjacent mediastinum and costal pleura. Sections of lung containing the irregularly circular nodules sank in formalin.

Laboratory Results:
Special stains:

Gram stain: The coccobacilli were Gram negative.

Bacteriology: Aerobic culture of the lungs yielded *Neisseria* sp. (predominant, 3+) and *Pasteurella* sp. (mixed, 2+) based on MALDI-TOF analysis.

Microscopic Description:

Slide B: Lungs – Widely-disseminated throughout all representative sections, affecting approximately 60-80% of the parenchyma, there are numerous, variably well demarcated nodules characterized by marked infiltration of the alveolar lumina, airways, and interstitium by degenerate and non-degenerate neutrophils admixed with abundant fibrin and large numbers of foamy macrophages. Within affected areas, alveolar septa are pale and indistinct to completely lost and replaced by large amounts of fibrin and proteinaceous and karyorrhectic debris (coagulative to lytic necrosis). Scattered bronchioles exhibit similar coagulative to lytic necrosis, with widespread sloughing and/or absence of bronchiolar epithelium. Numerous, large clusters of extracellular and occasionally in-
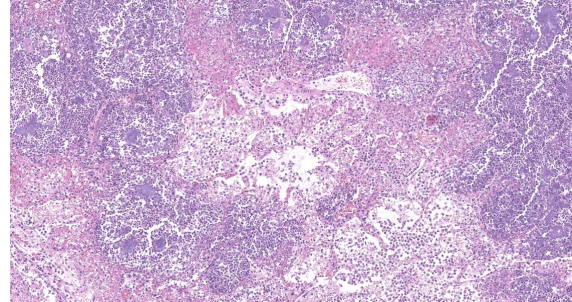
Figure 3-2. Lung, cat. There is extensive necrosis of the pulmonary parenchyma with septal necrosis, and filling of alveoli with fibrin, innumerable necrotic and viable neutropils, and large bacterial colonies. (HE, 108)

tra-neutrophilic and intra-histiocytic, basophilic, approximately 1um, coccobacilli are scattered throughout areas of inflammation and necrosis. Moderate to large numbers of extravasated erythrocytes are present in the alveolar lumina, airways, and interstitium multifocally (hemorrhage). Bronchiolar lumina are variably filled by large numbers of degenerate and non-degenerate neutrophils and macrophages, moderate numbers of sloughed epithelial cells, moderate numbers of coccobacilli, and large amounts of fibrin and cytoplasmic and nuclear debris. Blood vessels within nodules occasionally contain partially-occlusive to fully-occlusive thrombi
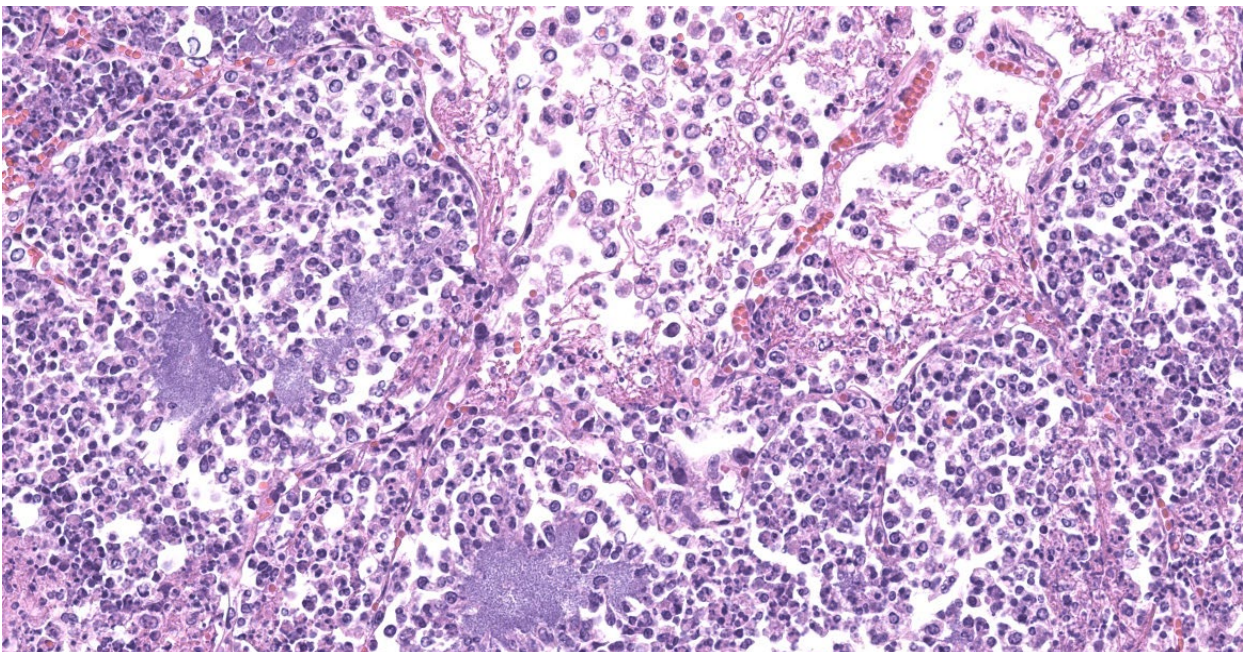
Figure 3-3. Lung, cat. Higher magnification of necrotic pulmonary parenchyma and alveolar contents. (HE, 367X)

with admixed degenerate and non-degenerate neutrophils and rare bacteria. The alveolar lumina between the nodules are filled by homogenous, eosinophilic material (edema) and contain small to moderate numbers of neutrophils and macrophages. Multifocally, mesothelial cells are plump (reactive) and the pleura is mildly to moderately thickened by small to moderate numbers of neutrophils and macrophages, and small amounts of fibrin and cellular debris.

Contributor's Morphologic Diagnoses:
1. Lungs:
   a. Pneumonia, necro-suppurative and histiocytic, multifocal, marked, acute with intralesional, intraneutrophilic, and intrahistiocytic bacteria, bronchitis, pleuritis, hemorrhage, and bacterial emboli.
   b. Alveolar edema, diffuse, marked, acute

Contributor's Comment:
Lower respiratory tract infection is an uncommon cause of morbidity and mortality in cats. Lower respiratory tract infections are often difficult to diagnose clinically due to nonspecific or inconsistent clinical, hematologic, and radiographic findings and concomitant respiratory or systemic pathology.[6] Reported infectious causes associated with feline pneumonia include bacteria, viruses, fungi, protozoa, rickettsia, and parasites, with *Bordetella bronchiseptica*, *Pasteurella* sp., *Mycoplasma* sp., *Streptococcus* sp., and *Escherichia coli*
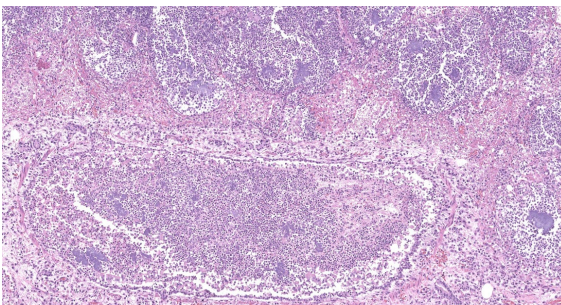
Figure 3-4. Lung, cat. Airways contain refluxed inflammatory cells and bacterial colonies. There is necrosis of airway epithelium and extension of inflammation into the peribronchiolar tissue. (HE, 367X)

considered the most common bacterial agents.[6]

Neisseria sp. bacteria are small, gram negative, coccobacilli, ecologically similar to *Pasteurella* sp. In human medicine, they are known as the causative agents of the sexually transmitted infection gonorrhea (*N. gonorrhoeae*), a form of bacterial meningitis (*N. meningitidis*), and uncommonly seen as secondary infection following feline and canine bite wounds (*N. animaloris* and *N. zoodegmatis*).[7,9] *Neisseria* sp. have been isolated as commensal flora from the oral cavity of healthy cats and dogs but are also a seldom reported cause of feline pneumonia.[6,7,9] Feline *Neisseria sp.* pneumonia was first described in 3 domestic cats in 1973, and sporadically thereafter in cases involving further domestic cats, a tiger cub, a lion, and Chinese leopard cats.[5,8,10,11]
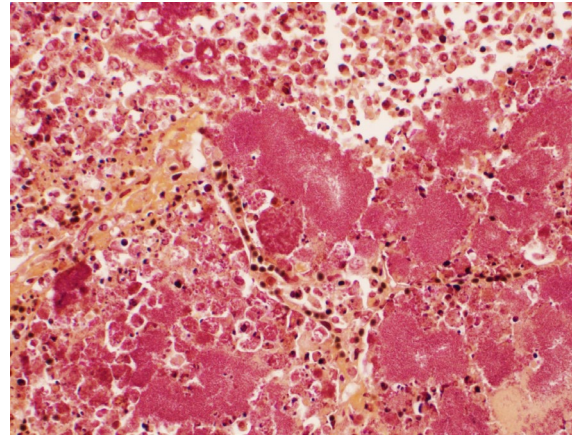
Cases of feline *Neisseria* sp. pneumonia are most commonly reported in adult cats, who present with variable clinical signs including acute depression, dehydration, respiratory distress, salivation, or sudden death.[3,6,8,10,11] Antemortem diagnostic testing results are also variable, with the most consistent finding being discrete, multifocal nodular densities and/or lung consolidation on thoracic radiographs.[6,8] Gross lesions consist of widespread, white to tan nodules scattered throughout the lung parenchyma, while the disease is histologically characterized by marked, multifocal, necrosuppurative and histiocytic, nodular pneumonia with abundant intralesional bacteria.[5,8,10,11]

While relatively unique, the reported radiographic, gross, and histologic findings are not considered pathognomonic for this entity without ancillary testing. Similar radiographic patterns have been reported in neoplasia and uncommonly secondary to other infectious causes, including but not limited to

Yersinia pestis, *Cryptococcus neoformans*, *Toxoplasma gondii*, *Mycoplasma* sp., *Mycobacterium* sp., and rarely other bacterial, fungal or parasitic causes.[3,6] While both *Neisseria* sp. and *Pasteurella* sp. bacteria were cultured from the lung in this case, *Pasteurella* sp. were considered less likely to be causing the primary disease, as these bacteria are common in the oral cavity and airways in healthy adult cats, are not uncommonly reported in mixed growth from feline pneumonia, and are generally associated with a suppurative bronchopneumonia when causing opportunistic lower respiratory tract disease.[2] In addition, multiple historic cases of feline nodular, necrosuppurative pneumonia, both in the literature and at our institution, have yielded pure growth of *Neisseria* sp. on aerobic culture.

The pathogenesis of feline *Neisseria* sp. pneumonia is not clear, but given the distribution and vascular bacterial emboli, is considered most likely secondary to hematogenous spread, potentially from the oral cavity.[8,11] The reason for the rare and severe nature of the disease given the oral commensal nature of some *Neisseria* species is not understood. One proposed mechanism is that chronic infection circumvents the host immune response, leading to a period of asymptomatic bacteremia and hematogenous spread to locations that favor survival and growth, with subsequent severe disease.[9] Immunosuppression has been hypothesized as a potential causative factor for pathogenesis in previous case reports, however, while this case exhibited marked neutropenia and lymphopenia, there was no evidence of other pathogenic processes leading to immunosuppression within the history, clinical, gross, or histologic findings.[5]

Unfortunately, prognosis is poor in *Neisseria* sp. pneumonia cases, with decline and death generally within hours to days of onset of

Figure 3-5. Lung, cat. Bacterial colonies are composed of large colonies of gram-negative cocci. (Brown-Hopps, 400X)

clinical signs, and only a single case report of successful feline *Neisseria* sp. pneumonia treatment.[6]

Contributing Institution:
Drs. Chris Bolt and Arno Wuenschmann
Minnesota Veterinary Diagnostic Laboratory
and Department of Population Medicine
University of Minnesota
1333 Gortner Ave.
St. Paul, MN 55108
www.vdl.umn.edu

JPC Diagnosis:
Lung: Pneumonia, necrotizing and fibrinosuppurative, diffuse, severe with thrombosis and large colonies of extracellular and intracellular cocci.

JPC Comment:
Neisseria animaloris and *Neisseria zoodegmatus* were previously known as Centers for Disease Control (CDC) Group Eugonic Fermenters (EF) 4a and 4b, respectively, until they were determined to belong to the *Neisseria* genus in 2006.[13] As the contributor states, *Neisseria* sp. are commensal organisms of the oral cavity of dogs and cats, and in addition to infrequently causing pneumonia, can rarely cause subcutaneous infections

of the neck and facial regions in cats. One report described a young adult Russian Blue cat with a submandibular mass characterized by necrosis, purulent inflammation, and fibrosis secondary to *Neisseria animaloris* (EF-4a at the time).[1] In a separate report, a young adult domestic short hair cat developed subcutaneous swelling over the bridge of the nose due to pyogranulomatous inflammation and *Neisseria* sp infection.[4] Routine stains did not illustrate bacteria in the first case; however, in the second case, gram-negative, non-acid-fast coccobacilli with a PAS-positive capsule were identified within macrophages. Both cases responded to debulking and antibiotic therapy, and traumatic inoculation from penetrating injury were suspected to be the initial cause of infection.[1,4]

As the contributor mentioned, *N. meningitidis* and *N. gonorrhoeae* are significant pathogens in humans. While most Gram-negative bacteria use siderophores to obtain iron, pathogenic (non-commensal) *Neisseria* species have evolved a unique mechanism to extract iron from host serum transferrin (TF), the predominant mammalian transport protein for iron.[12] The bacterial transferrin receptor consists of two parts: TF-binding protein B (TbpB, a surface lipoprotein), which initially harnesses TF, and TF-binding protein A (Tbp A, a TonB-dependent transporter), which removes and transports ferric acid into the bacteria through a conformationally-active pore.[12] While the majority of research on Tbps has been conducted in Neisseria species, similar receptors have been found in Pasteurellaceae and Moraxellaceae species, including *Actinobacillus pleuropneumoniae* and *Histophilus somni*.[12] Bacterial Tbp activity appears to be host-species specific and increases pathogen virulence within the host.

References:

1. Baral RM, Catt MJ, Soon L, et al. Successful treatment of a localized CDC group EF-4a infection in a cat. *J Feline Med Surg*. 2017;9(1):67-71.
2. Bart, M et al. Feline Infectious Pneumonia: A Short Literature Review and a Retrospective Immunohistological Study on the Involvement of Chlamydia spp. and Distemper Virus. *The Veterinary Journal*. 2000; 159:220-230.
3. Carniel F et al. What Is Your Diagnosis? *J Am Vet Med Assoc*. 2020; 257(4):375-377.
4. Carr SV, Martin PA, Keyes L, Tong LJ, Talbot JJ, Muscatello G, Barrs VR. Nasofacial infection in a cat due to a novel bacterium in *Neisseriaceae*. *JFMS Open Rep*. 2015;1(2):1-5.
5. Ceyssens et al. Necrotizing Pneumonia in Cats Associated with Infection of EF-4a Bacteria. *J Vet Med*. 1989; 36(4):314-316.
6. Foster S, Martin P. Lower Respiratory Tract Infections in Cats - Reaching beyond empirical therapy. *J Feline Med Surg*. 2011; 13(5):313-332.
7. Heydecke A et al. Human wound infections caused by *Neisseria animaloris* and *Neisseria zoodegmatis*, former CDC Group EF-4a and EF-4b. *Infection Ecology and Epidemiology*. 2013; 3: 20312.
8. Jang SS et al. Focal Necrotizing Pneumonia in Cats Associated with a Gram Negative Eugonic Fermenting Bacterium. *Cornell Vet*. 1973; 63:446-454
9. Liu G et al. Non-Pathogenic *Neisseria*: members of an abundant, multi-habitat, diverse genus. *Microbiology*. 2015; 161:1297-1312
10. Lloyd J, Allen JG. The isolation of Group EF-4 bacteria from a case of granulomatous pneumonia in a tiger cub. *Aust Vet J*. 1980; 56(8):399–400.
11. Perry AW, Schlingman DW. Pneumonia Associated with Eugonic Fermenter-4 Bacteria in Two Chinese Leopard Cats. *Can Vet J*. 1988; 29(11): 921-922.

12. Pogouste AK, Morales TF. Iron acquisition through the bacterial transferrin receptor. *Crit Rev Biochem Mol Biol.* 2017: 52(3):314-326.
13. Vandamme P, Holmes B, Bercovier H, Coenye T. Classification of Centers for Disease Control Group Eugonic Fermeter (EF)-4a as *Neisseria animaloris* sp. nov. and *Neisseria zoodegmatis* sp. nov, respectively. *Int J Syst Evol Microbiol.* 2006:56(Pt8):1801-1805.

CASE IV:

Signalment:
1-year-old female Wyandotte chicken (*Gallus gallus*)

History:
This chicken was lethargic, diarrheic and was losing weight. She was found laterally recumbent with her right leg extended behind her and the left leg curled underneath her. Coelomocentesis revealed yellow coelomic fluid. Euthanasia was elected, and the carcass was received for examination. This chicken was part of a small backyard flock of 16 chickens.

Gross Pathology:
The chicken was in poor body condition with scant visceral fat and moderate pectoral muscle atrophy. There was approximately 100 mL of yellow, turbid, watery fluid within the coelomic cavity. Multifocally throughout the walls of the small intestine and large intestine, and occasionally extending into the lumen, were dozens of semi-firm, pale tan-yellow nodules which ranged from 0.3 to 2 cm in diameter. On cut section, these nodules were pale tan and bulged slightly. The mesentery was tan and diffusely moderately thickened.

Laboratory Results:
Qualitative fecal analysis: Few *Capillaria* sp. eggs, few *Heterakis* sp. eggs, few coccidial oocysts

Microscopic Description:
Small intestine: Diffusely expanding and effacing the serosa of the small intestine and the surrounding mesentery is a poorly demarcated, highly cellular proliferation of neoplastic round cells. Neoplastic cells are arranged in sheets and supported by collagenous stroma. Neoplastic cells are round with distinct cell borders and have small to moderate amounts of eosinophilic cytoplasm. Nuclei are round, finely stippled to vesiculate and have 1-3 nucleoli. There is moderate anisocytosis and anisokaryosis and 43 mitoses in 10 high-power fields (400x). Multifocally, neoplastic cells infiltrate the small intestinal muscularis and submucosa. The adjacent pancreas is extensively obscured to effaced by similar neoplastic cells.

Figure 4-1. Small intestine, chicken. There are dozens of multifocal to coalescing semi-firm, tan-yellow, 0.3-2 cm diameter nodules throughout the walls of the small intestine, mesentery and pancreas. (Photo courtesy of NIH Comparative Biomedical Scientist Training Program, National Cancer Institute, https://nih-cbstp.nci.nih.gov/)

Immunohistochemistry:
The neoplastic round cells within the small intestine, mesentery and pancreas exhibit strong perimembranous immunoreactivity for CD3, strong nuclear immunoreactivity for Meq and are not immunoreactive for BLA.36.
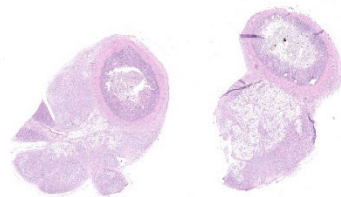
Contributor's Morphologic Diagnoses:
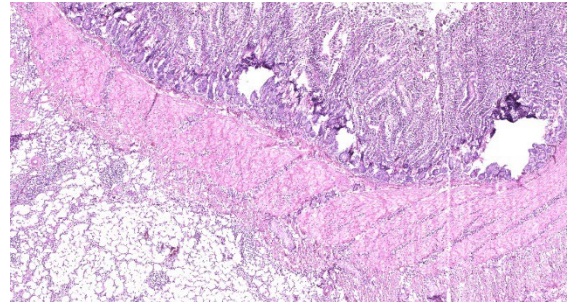Small intestine: T-cell lymphoma
Pancreas: T-cell lymphoma

Contributor's Comment:
The histopathologic findings are consistent with visceral lymphoma, which in this case was immunohistochemically confirmed as Marek's disease using antibodies directed against the Marek's disease virus Meq protein.

Marek's disease (MD) in chickens occurs upon inhalation of gallid alphaherpesvirus-2, a cell-associated alphaherpesvirus with lymphotropic properties similar to gammaherpesviruses.[13] Marek's disease virus (MDV) is a member of the genus Mardivirus and are divided into three serotypes: Gallid herpesvirus 2 (MDV-1), Gallid herpesvirus 3 (MDV-2), and Meleagrid herpesvirus 1 (MDV-3). Of these three serotypes, only MDV-1 causes disease in chickens.[13,15] Strains of MDV are classified into four pathotypes based on their virulence, referred to as mild (m), virulent (v), very virulent (vv)


Figure 4-3. Small intestine and mesentery. A moderately cellular round cell neoplasm transmurally infiltrates the intestine and extends into the adjacent mesentery. (HE, 49X)

Figure 4-2. Small intestine and mesentery. Two sections of intestine and mesentery (one with pancreas) are submitted for examination. At subgross, the mesentery and intestine contain a dense cellular exudate. (HE, 5X)

and very virulent plus (vv+) strains.[1,13] The m strains can cause mild neurological disease, the v and vv strains can cause lymphomas, and the vv+ strains can cause fatality with severe brain edema and tumors in unvaccinated and vaccinated chickens.[1,15]

Previously, MDV posed a serious economic threat causing up to 60% mortality in layer flocks, and currently exists in all poultry-producing countries.[2,13,14] Despite the more recent advent and widespread use of a live-attenuated vaccine, sporadic losses still occur on individual farms, and the disease is still a concern in poultry flocks.[13] Concerns of the vaccine selecting for MDV strains of higher virulence also exist, as MDV vaccines prevent clinical signs but do not prevent virus replication and shedding in vaccinated chickens.[1,14] Nearly all chickens can be infected by MDV and develop tumors, and turkeys, quail, and pheasants are also susceptible to infection and disease.[13] Marek's disease outbreaks may occur in unvaccinated chickens as young as 3-4 weeks, although most serious cases begin after 8-9 weeks of age.[13]

The pathogenesis of MDV infection in vivo is divided into four stages.[15] In the early cytolytic phase, B cells undergo cytolytic infection.[15] In the latency phase, MDV infects CD4+ and CD8+ T-cells.[15] Following MDV reactivation in CD4+ T-cells, a late cytolytic
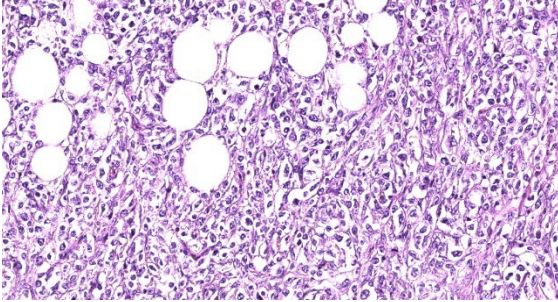
Figure 4-4. Mesentery, chicken. Neoplastic cells infiltrate and efface the mesentery. (HE, 381X)

and immunosuppressive phase is initiated.[15] Finally, the transformation phase occurs and is characterized by the development of CD4+ T-cell lymphomas.[15]

Marek's disease can manifest as distinct lymphoproliferative syndromes, such as lymphomas, cutaneous leukosis, atherosclerosis, early mortality, cytolytic syndromes, immunosuppression, and lymphoproliferation in the eyes and CNS as well as peripheral nerves resulting in "fowl paralysis".[13] Gross lesions associated with MD may include unilaterally gray or yellow, edematous, and enlarged peripheral nerves, such as the sciatic and brachial nerves, which may be 2 to 3 times normal size.[13] Lymphomas may also occur in virtually all visceral organs, including the mesentery, intestine, pancreas, kidney, liver, spleen, bursa of Fabricius, thymus, iris ("gray eye"), feather follicles, heart, muscle and gonads, particularly the ovary.[13] Visceral tu mors may appear as gray or yellow firm nodules or diffuse organ enlargements.[13] In this case, differential diagnoses for the gross lesions would include avian tuberculosis or Hjarre's disease (coligranuloma), which were later ruled-out with microscopic examination.

Microscopic lesions within visceral organs correspond to proliferations of monomorphic neoplastic small to large T-cells, lymphoblasts and mononuclear inflammatory infiltrates.[13] Within peripheral nerves, lymphoproliferative lesions are separated into

types A and B.[3,13] Type A lesions are neoplastic and consist of T-cells and fewer B-cells.[3,13] Type B lesions are inflammatory and are characterized by mononuclear cell infiltrates composed of small lymphocytes and plasma cells and fewer macrophages.[3,13]

In the current case, only lymphoma affecting visceral organs was appreciated. In addition to infiltrating and obliterating the intestinal walls, mesentery, and pancreas, similar neoplastic lymphocytes extensively effaced the ovary and infiltrated the splenic capsule.

The primary differential diagnoses for lymphoma in chickens include Marek's disease, and the retroviruses avian leukosis virus (ALV) and reticuloendothelial virus (REV).[7,13] Immunophenotyping with T- and B-cell markers can help to distinguish between MDV and ALV, as MDV commonly induces T-cell lymphomas, while ALV induces B-cell lymphomas.[7] In the current case, neoplastic cells exhibited strong perimembranous labeling for the T-cell marker CD3 and were negative for the B-cell marker BLA.36. PCR may also be used to identify the presence of MDV.[6,7,11]
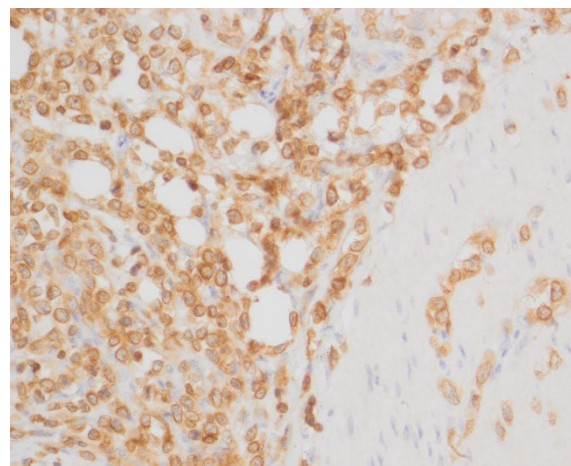
Figure 4-5. Small intestine, chicken. Neoplastic lymphocytes exhibit strong perimembranous immunoreactivity for CD3 (anti-CD3, 400X). (Photo courtesy of NIH Comparative Biomedical Scientist Training Program, National Cancer Institute, https://nih-cbstp.nci.nih.gov/)

In addition, immunohistochemistry using antibodies directed against the MDV-specific viral antigens Meq and pp38 can be used to help confirm a diagnosis of MD. Meq (Marek's EcoQ) is a leucine zipper regulatory protein similar to the Fos and Jun oncoproteins, and has been demonstrated to be critical to MD oncogenesis.[10,14] The functions of Meq include DNA binding, chromatin remodeling and regulation of transcription.[14] Meq can form homodimers or heterodimers with proto-oncoproteins, such as c-Myc, c-Fos, ATF and c-Jun. Meq can also bind to and sequester RB, p53 and cyclin-dependent kinase 2 (CDK2), leading to dysregulated cell-cycle control and the oncogenic transformation of T-cells.[14] The exact biological function of pp38 is currently unknown, but has been associated with lymphoid tropism, oncogenicity, reactivation from latency, viral replication in the early lytic phase and maintenance of transformation in MDV-infected tumor cells.[8] Meq has been shown to be the only viral antigen consistently expressed, but pp38 positive cells may also be observed.[7] In our case, the neoplastic T-cells exhibited strong nuclear immunoreactivity for Meq but were not immunoreactive for pp38.

Contributing Institution:
NIH Comparative Biomedical Scientist Training Program, National Cancer Institute
https://nih-cbstp.nci.nih.gov/

JPC Diagnoses:
1. Small intestine, mesentery, pancreas: Lymphoma.
2. Small intestine, lumen: Cestode adult.

JPC Comment:
In 1907, Hungarian veterinarian Jozsef Marek described a syndrome of polyneuritis in chickens termed fowl paralysis and now known as Marek's disease.[1] In 1967, the her-

pesviral etiology was discovered. Observations that the virus spread via indirect contact and remained infectious in the environment for months led to further research into the transmission of the virus, and in 1970, Calnek et al. described enveloped herpesvirus particles in the feather follicular epithelium that were infectious to and produced Marek's disease in other chickens.[4] Since then, cell-free virions produced in the feather follicle epithelium and shed in feathers and dander of infected birds have been recognized as the source of horizontal transmission.

The economic impact of Marek's disease is estimated to be up to $2B USD annually, with losses stemming from decreased productivity, immunosuppression leading to comorbidities, and aesthetic condemnation at slaughter.[1,5,12] As such, tremendous research has gone into developing prevention and control methods, and there are currently three main lines of effort: selecting for genetically resistant chickens, improving biosecurity to prevent spread between flocks, and vaccination. Several Marek's disease virus (MDV) vaccinations have been developed, including a vaccine using herpesvirus of turkeys and attenuated MDV strains SB1 and CVI988.[5]
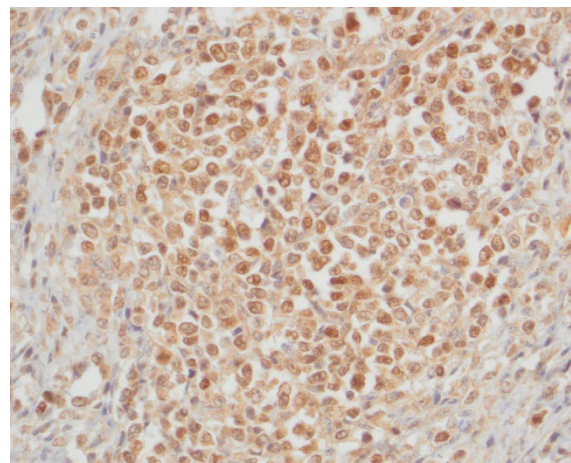
Figure 4-6. Small intestine, chicken. Neoplastic lymphocytes exhibit nuclear immunoreactivity for Meq (anti-Meq, 400X). (Photo courtesy of NIH Comparative Biomedical Scientist Training Program, National Cancer Institute, https://nih-cbstp.nci.nih.gov/)

While these vaccines are generally effective in preventing clinical disease in vaccinated birds, they do not produce sterile immunity, and vaccinated birds can still be infected and shed the virus. This has selected for and supported the spread of more virulent strains of MDV that would, in unvaccinated populations, be self-limiting in scope due to their high mortality rates. [1,5,12]

Recent research has uncovered one key component of MDV transmission: conserved herpesvirus protein kinase (CHPK).[9] CHPKs are encoded by all members of the Herpesviridae family and support a variety of functions throughout viral infection stages (such as nuclear egress and viral DNA replication).[9] In MDV, CHPK is not required for cell-to-cell transmission or progression of clinical disease, but it is specifically required for horizontal transmission.[9] Recent studies indicate that CPHK is most likely integral for production of cell-free virions, as mutated CPHK results in defects in the viral replication pathway in feather follicular epithelium, but CPHK's role in establishing infections in new individuals has not been ruled out.[9] In either case, this research provides insight into the horizontal transmission of MDV which has yet to be overcome by vaccination strategies.

References:

1. Bertzbach LD, Conradie AM, You Y, Kaufer BB. Latest insights into Marek's disease virus pathogenesis and tumorigenesis. *Cancers*. 2020;12(3):647.
2. Boodhoo N, Gurung A, Sharif S, Behboudi S. Marek's disease in chickens: a review with focus on immunology. *Veterinary research*. 2016;47(1):1-9.
3. Burgess SC, Basaran BH, Davison TF. Resistance to Marek's disease herpesvirus-induced lymphoma is multiphasic and dependent on host genotype. *Veterinary Pathology*. 2001;38(2):129-42.
4. Calnek BW, Adldinger HK, Kahn DE. Feather follicle epithelium: A source of enveloped and infectious cell-free herpesvirus from Marek's disease. *Avian Dis.* 1970; 14:219-233.
5. Davidson I. Out of Sight, but Not Out of Mind: Aspects of the Avian Oncogenic Herpesvirus, Marek's Disease Virus. *Animals*. 2020; 10: 1319-1332.
6. Gimeno IM, Dunn JR, Cortes AL, El-Gohary AE, Silva RF. Detection and differentiation of CVI988 (Rispens vaccine) from other serotype 1 Marek's disease viruses. *Avian diseases*. 2014;58(2):232-43.
7. Gimeno IM, Witter RL, Fadly AM, Silva RF. Novel criteria for the diagnosis of Marek's disease virus-induced lymphomas. *Avian Pathology*. 2005;34(4):332-40.
8. Gimeno IM, Witter RL, Hunt HD, Reddy SM, Lee LF, Silva RF: The pp38 Gene of Marek´s Disease Virus (MDV) Is Necessary for Cytolytic Infection of B Cells and Maintenance of the Transformed State but Not for Cytolytic Infection of the Feather Follicle Epithelium and Horizontal Spread of MDV. *Journal of Virology* 2005;79(7):4545-4549.
9. Krieter A, Ponnuraj N, Jarosinski KW. Expression of the Conserved Herpesvirus Protein Kinase (CHPK) of Marek's Disease Alphaherpesvirus in the Skin Reveals a Mechanistic Improtance for CHPK during Interindividual Spread in Chickens. *J Virol*. 2020; 95(5):1-12.
10. Lupiani B, Lee LF, Cui X, Gimeno I, Anderson A, Morgan RW, Silva RF, Witter RL, Kung HJ, Reddy SM. Marek's disease virus-encoded Meq gene is involved in transformation of lymphocytes but is dispensable for replication. *Proceedings of the National Academy of Sciences*. 2004;101(32):11815-20.
11. Mete A, Gharpure R, Pitesky ME, Famini D, Sverlow K, Dunn J. Marek's disease in

backyard chickens, a study of pathologic findings and viral loads in tumorous and nontumorous birds. *Avian diseases*. 2016;60(4):826-36.

12. Nair V. Spotlight on avian pathology: Marek's Disease. *Avian Path.* 2018; 47(5):440-442.

13. Nair V, Gimeno I, Dunn J. Neoplastic diseases: Marek's disease. In: Swayne DE, ed. *Diseases of Poultry*. 14th ed. Wyley-Blackwell. 2020.

14. Osterrieder N, Kamil JP, Schumacher D, Tischer BK, Trapp S. Marek's disease virus: from miasma to model. *Nature Reviews Microbiology*. 2006;4(4):283-94.

15. Shi MY, Li M, Wang WW, Deng QM, Li QH, Gao YL, Wang PK, Huang T, Wei P. The emergence of a vv+ MDV can break through the protections provided by the current vaccines. *Viruses*. 2020;12(9):1048.